Evaporation, infiltration and storage of soil water in different vegetation zones in the Qilian Mountains: A stable isotope perspective

Guofeng Zhu [1,2], Leilei Yong [1,2], Xi Zhao [1,2], Yuwei Liu [1,2], Zhuanxia Zhang [1,2], Yuanxiao Xu [1,2], Zhigang Sun [1,2], Liyuan Sang [1,2], Lei Wang [1,2]

[1] College of Geography and Environment Science, Northwest Normal University, Lanzhou 730070, China

[2] Shiyang River Ecological Environment Observation Station, Northwest Normal University, Lanzhou 730070, Gansu, China

Correspondence to: Guofeng Zhu (zhugf@nwnu.edu.cn)

Abstract: The processes of water storage have not been fully understood in different vegetation zones in mountainous areas, which is the main obstacle to further understanding hydrological processes and improving water resource assessments. To further understand the process of soil water movement in different vegetation zones (alpine meadow, coniferous forest, mountain grassland, and deciduous forest) in mountainous areas, this study monitored the temporal and spatial dynamics of hydrogen and oxygen stable isotopes in the precipitation and soil water of the Xiying River Basin. The results show that the order of soil water evaporation intensities in the four vegetation zones was mountain grassland (SWL_{slop}: 3.4) > deciduous forest (SWL_{slop}: 4.1) > coniferous forest (SWL_{slop}: 4.7) > alpine meadow (SWL_{slop}: 6.4). The soil water in the alpine meadow and coniferous forest evaporated from only the topsoil, and the rainfall input was fully mixed with each layer of soil. The evaporation signals of the mountain grassland and deciduous forest could penetrate deep into the middle, and lower layers of the soil as precipitation quickly flowed into the deep soil through the soil matrix. Each vegetation zone's water storage capacity of the 0-40 cm soil layer followed the order of alpine meadow (46.9 mm) > deciduous forest (33.0 mm) > coniferous forest (32.1 mm) > mountain grassland (20.3 mm). In addition, the 0-10cm soil layer has the smallest soil water storage capacity (alpine meadow:43.0 mm; coniferous forest: 28.0 mm; mountain grassland: 17.5 mm; deciduous forest:

30 29.1 mm). This work will provide a new reference for understanding soil hydrology in

31 arid headwater areas.

32 **Key words:** Xiying River; Stable isotope; Drought, Soil water storage

1. Introduction

34   In arid inland river basins, climate and vegetation changes will affect the

35 hydrological cycle (Sharma et al., 2021; Tetzlaff et al., 2013). As an essential part of

36 the water cycle, soil water in the unsaturated zone can be converted from precipitation

37 into the stream or groundwater recharge. Determining soil water's evaporation,

38 infiltration, and storage properties are critical to understand the regional hydrological

39 cycle and water balance under climate and vegetation changes (Brooks et al., 2010;

40 Dubbert and Werner, 2019; Grant and Dietrich, 2017).

41   As "fingerprints" of water, isotopes have been used to track ecohydrological

42 characteristics, such as evaporation (Barnes and Allison, 1988; Zhu et al., 2021b),

43 groundwater recharge (Koeniger et al., 2016), infiltration paths (Duvert et al., 2016;

44 Tang and Feng, 2001; Zhu et al., 2021a), evapotranspiration distribution (Gibson et al.,

45 2021; Xiao et al., 2018), and the water absorption by plants (Rothfuss and Javaux,

46 2017).

47   Water seepage in the unsaturated soil zone and water evaporation at the air–soil

48 interface are the primary forms of soil water transport. The dynamic water process

49 reflected by the displacement of the isotope signal on the soil profile is called the

50 "memory effect". Understanding the "memory effect" will help us to trace the

51 dynamic changes in climate and soil hydrology (Kleine et al., 2020). The change of

52 stable isotopes in near-surface soil water may reflect the precipitation variation, but

53 these variations decrease with depth unless there is preferential flow (Peralta-Tapia et

54 al., 2015; Sprenger et al., 2016; Sprenger et al., 2017). Evaporation mainly occurred

55 in the near-surface part of the soils (0-10 cm), and the light isotope molecules (^{1}H and

56 ^{16}O) evaporated preferentially, resulting in the enrichment of heavy isotopes (^{2}H and

57 ^{18}O) on the soil surface (Ferretti et al., 2003). Dansgaard (1964) proposed the concept

58 of d-excess (d-excess=δ^2H-8δ^{18}O) to illustrate the intensity of evaporation

fractionation. Assuming that evaporation occurs in the atmosphere with a humidity of 75%, it shows that the d-excess value of atmospheric moisture accounts for the d-excess value of 10‰ in the atmospheric moisture, which conforms to the worldwide average isotopic labelling of meteoric waters. Landwehr and Coplen (2006) defined line conditioned excess as the difference between the δ^2H value of the water sample and the $\delta^{18}O$ linear transform value of the same sample, where the linear transformation reflects the relevant referenced meteoric water relationship. Compared with d-excess, lc-excess can explain the evaporative fractionation process better. The main reason is that lc-excess of precipitation and soil water changes smoothly and has relatively small seasonal changes (Landwehr et al., 2014). The dynamic changes of isotopes record the signal of soil water evaporation. This enrichment of this dynamic fractionation exists in soil water isotopes in different climatic regions. Compared with temperate regions, the evaporation signals in arid and Mediterranean environments penetrate deeper into the soil (Sprenger et al., 2016). After evaporation and seepage, some water is stored in the soil . The water storage capacity in humid areas is higher than that in arid areas, that in forest is higher than that in grassland, and that in surface soil layer is lower than that in deep soil layers with high clay content (Kleine et al., 2020; Milly, 1994; Snelgrove et al., 2021; Sprenger et al., 2019).

In alpine mountains, climate warming has accelerated the melting of glaciers and frozen soil, and the dynamic interaction between water bodies stored in different media has become the main influencing factor of the water cycle (Penna et al., 2018). Interactions between precipitation and the soil-plant-atmosphere system determine the distribution of water in various storage reservoirs and the subsequent release of water vapor to the atmosphere. These interactions include mainly interception, throughfall, canopy drip, snow accumulation and ablation, infiltration, surface and subsurface runoff, soil moisture, and the partitioning of evapotranspiration between canopy evaporation, transpiration, and soil evaporation. As the main links of the hydrological cycle, these processes have a profound impact on regional water balance and flux distribution.

In the past, studies on the evaporation, infiltration and storage of soil water mostly focused on vegetation types in the same climatic region or different climatic regions. Understanding the climatic and hydrological conditions of different vertical vegetation zones and clarifying the regulating role of vegetation in the water cycle can help better adapt to climate change's influences on the hydrological cycle in source areas. In this study, we monitored the stable isotope composition of precipitation and soil water and the spatio-temporal dynamics of soil water storage in four vegetation zones (alpine meadow, coniferous forest, mountain grassland, and deciduous forest) at different temperatures and humidity in the Xiying River basin. To explore the differences in soil water evaporation, infiltration, and storage processes in these four different climates, vegetation types, and terrain types, the following research objectives were proposed: (1) to explore the evolution of isotope evaporation signals and the "memory effects" of precipitation input, mixing and rewetting; (2) to understand the soil water storage capacity and influencing factors of four vegetation areas in mountainous areas. It is hoped that this study can further improve the understanding of the water cycle process and provide a scientific theoretical reference for water resource utilization and ecological restoration in fragile environments. More importantly, it can provide paradigms for research at different spatial scales (latitude zone, longitude zone, watershed, etc.) based on the knowledge of soil moisture evaporation, infiltration, and water storage in typical vertical vegetation zones.

2. Study area

The Xiying River originates from Lenglongling and Kawazhang in the eastern Qilian Mountains (101°40′47″~102°23′5″E, 37°28′22″~38°1′42″N) (Fig. 1). As the largest tributary of the Shiyang River, it is formed by the Shuiguan River, Ningchang River, Xiangshui River, and Tatu River converging from southwest to northeast and ultimately flowing into the Xiying Reservoir. The average annual runoff of the Xiying River is 388 million m^3, which is mainly replenished by mountain precipitation and melting water of ice and snow. The runoff is mainly concentrated in summer. The basin elevation is between 2000 m and 5000 m, corresponding to a

temperate semiarid climate with strong solar radiation, a long sunshine time, and a large temperature difference between day and night. The average annual temperature of the basin is 6°C, the annual average evaporation is 1133 mm, the annual average precipitation is 400 mm, and the precipitation from June to September accounts for 69% of the annual precipitation. Precipitation increases with elevation, while temperature decreases with elevation in this area (Table 1) (Ma et al., 2018). The zonal differentiation of vegetation in the basin is dominated by deciduous forest, mountain grassland, cold temperate coniferous forest, and alpine meadow. The soils mainly include lime, chestnut, alpine shrub meadow, and desert soil (Fig. 1).
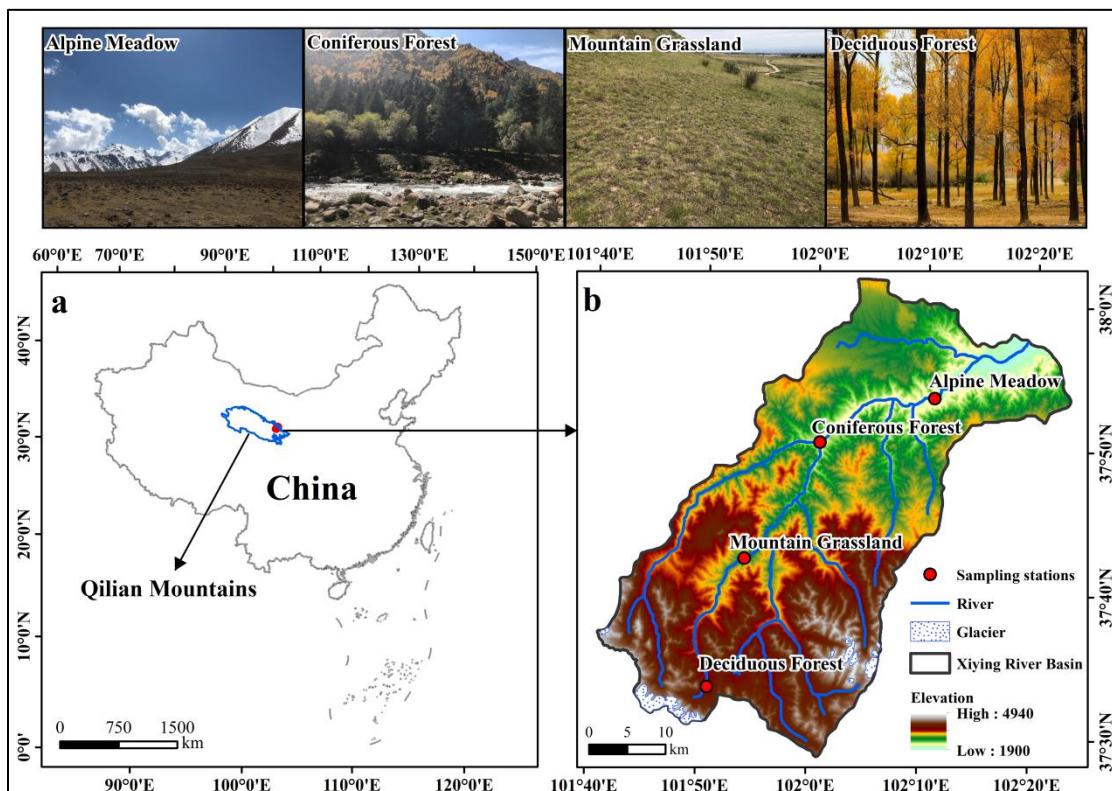
Fig. 1 Study area and location of sampling points(a. The location of the Xiying River Basin in China; b. The terrain and sampling points of the Xiying River Basin)

3. Data and methods

3.1 Sample collection

In this study, soil water and precipitation samples were collected from four vegetation zones in the Xiying River basin from April to October in 2017 (plant growing season). In 2017, the precipitation in the alpine meadow, coniferous forest, mountain grassland and deciduous forest were 595.1 mm, 431.9 mm, 363.5 mm and

262.5 mm, respectively. The average daily temperatures in the alpine meadow, coniferous forest, mountain grassland and deciduous forest were -0.19℃, 3.34℃, 6.6℃ and 7.9℃, respectively (Table 1).

Collection of soil samples: Soil samples were collected once a month at depths of 0-10, 10-20, 20-30, 30-40, 40-50, 50-60, 60-70, 70-80, 80-90, and 90-100 cm from the soil layers in the four vegetation zones. Three duplicate samples were collected for each soil layer. We placed the collected soil sample into a 50 mL glass bottle, sealed the bottle mouth with Parafilm and marked the sampling date. We froze the sample for storage until experimental analysis. Each sample was collected separately in an aluminum box.

Collection of precipitation samples: The precipitation samples were collected by a plastic funnel bottle device. After each precipitation event, the collected precipitation samples were immediately transferred to an 80 mL high-density polyethylene bottle, and the bottle mouth of the samples was sealed with Parafilm; these samples were also frozen and stored until experimental analysis.

Meteorological data: During the sampling period, the local meteorological data were obtained and recorded by automatic weather stations (Watchdog 2000 series weather stations) set up near the sample plot.

Table 1 Basic data of each Vegetation zone from April to October 2017 (*Long*-Longitude, *Lat*-Latitude, *Alt*-Altitude, *T*-Air Temperature (daily mean temperature), *P*-Precipitation (total precipitation during the observation period), *h*-Relative Humidity (daily mean relative humidity))

Vegetation zone	Geographical parameters			Meteorological parameters			Number of samples	
	Long(°E)	*Lat*(°N)	*Alt*(m)	*T*(℃)	*P*(mm)	*h*(%)	Precipitation	Soil
Alpine Meadow	101°51'16"	37°33'28"	3637	-0.19	595.1	69.2	72	47
Coniferous Forest	101°53'23"	37°41'50"	2721	3.34	431.9	66.6	42	41
Mountain Grassland	102°00'25"	37°50'23"	2390	6.6	363.5	60.4	37	54
Deciduous Forest	102°10'56"	37°53'27"	2097	7.9	262.5	59.8	40	53

3.2 Sample determination

157   The analysis of δ^2H and $\delta^{18}O$ values of all the above water samples was

158   completed using a liquid water isotope analyzer (DLT-100, Los Gatos Research, USA)

159   in the stable isotope laboratory of Northwest Normal University. Before analyzing the

160   isotope values of soil water, the soil water was extracted from the collected soil

161   samples by a low-temperature vacuum condensation system (LI-2100, LICA United

162   Technology Limited, China). Both the water and isotope standard samples were

163   injected 6 times during the analysis. To avoid the "memory effect" of isotope analysis,

164   we discarded the first two injection values and used the average value of the last four

165   injections as the final result (Penna et al., 2012; Qu et al., 2020). The analysis results

166   were relative to VSMOW (Vienna Standard Mean Ocean Water):

$$\delta = \left(\frac{R_{\text{sample}}}{R_{\text{standard}}} - 1 \right) \times 1000\text{‰} \tag{1}$$

167   where R_{sample} is the ratio of $^{18}O/^{16}O$ or $^2H/^1H$ in the sample and $R_{standard}$ is the ratio of

168     $^{18}O/^{16}O$ or $^2H/^1H$ in the VSMOW. The test error of the δ^2H value does not exceed

169   ± 0.6‰, and the test error of the $\delta^{18}O$ value does not exceed ± 0.2‰.

170   **3.3 Analysis method**

171   **3.3.1 Lc-excess**

172   The linear relationship between δ^2H and $\delta^{18}O$ in precipitation and soil water is

173   defined as the LMWL (local meteoric water line) and SWL (soil waterline),

174   respectively, which are of great significance for studying the evaporative fractionation

175   of stable isotopes during the water cycle. We further calculated the line-conditioned

176   excess for each soil water and precipitation sample. The lc-excess in different water

177   bodies can characterize the evaporation index of different water bodies relative to the

178   local precipitation (Landwehr and Coplen, 2006).

$$\text{lc} - \text{excess} = \delta^2H - a \times \delta^2H - b \tag{2}$$

179   where a and b are the slope and intercept of the LMWL, respectively, and δ^2H and

180     $\delta^{18}O$ are the isotopic values of hydrogen and oxygen in the sample. The physical

181   meaning of lc-excess is expressed as the degree of deviation of the isotope value in

182   the sample from the LMWL, indicating the nonequilibrium dynamic fractionation

183 process caused by evaporation. Generally, the change in lc-excess in local

184 precipitation is mainly affected by different water vapor sources, and the annual

185 average is 0. Since the stable isotopes in soil water are enriched by evaporation, the

186 average lc-excess is usually negative (Landwehr et al., 2014; Sprenger et al., 2017).

187 **3.3.2 Potential evapotranspiration**

188 The potential evapotranspiration was calculated based on the Penman-Monteath

189 equation (Allen, 1998):

$$PET = \frac{0.408\Delta(R_n - G) + \gamma \frac{900}{T+273} u^2 (e_s - e_a)}{\Delta + \gamma(1 + 0.34u^2)} \tag{3}$$

190 where PET is the daily potential evapotranspiration (mm day^{-1}), R_n is the net radiation

191 (MJ m^2 day^{-1}), G is the soil heat flux density (MJ m^2 day^{-1}), γ is the psychrometric

192 constant (kPa°C^{-1}), u_2 is the wind speed at 2 m height (m s^{-1}), T is the mean daily air

193 temperature at 2 m height (°C), Δ is the slope of the vapor pressure curve (kPa°C^{-1}), e_a

194 is the actual vapor pressure (kPa) and e_s is the saturated vapor pressure (kPa). These

195 data come from nearby weather stations.

196 **3.3.3 Soil water storage**

197 Soil water storage is the thickness of the water layer formed by all the water in a

198 certain soil layer (Milly, 1994) and is expressed by the following formula:

$$S = R \times W \times H \times 10 \tag{4}$$

199 where S is the soil water storage in a certain thickness layer (mm), R is the soil bulk

200 density (g cm^{-3}), and H is the soil thickness (cm). W is the gravimetric water content,

201 which is expressed by the following formula:

$$W = \frac{M_1 - M_2}{M_2} \times 100\% \tag{5}$$

202 in the formula, M_1 is the gravimetric value of wet soil (g), and M_2 is the gravimetric

203 value of dry soil (g).

4. Results and analysis

4.1 Hydrological climate

PET and runoff are important indicators that reflect the dry-wet conditions of river basins. During the study period (April-October 2017), in the Xiying River Basin, the potential evapotranspiration was 872.8 mm, the daily evapotranspiration ranged from 7.5 mm (July 14) to 0.9 mm (October 9), showing a fluctuating trend around July, and the PET value in April-July was higher than that in August-October. The input of summer precipitation and ice/snow meltwater increased runoff, resulting in a trend similar to PET. During the observation period, the total runoff was 3.1×10^9 m, accounting for 89% of the annual runoff. The variation range of the daily runoff was 286848 m³ (April 17) to 6125760 m³ (July 13). The basin before July was drier than that after July (Fig. 2).
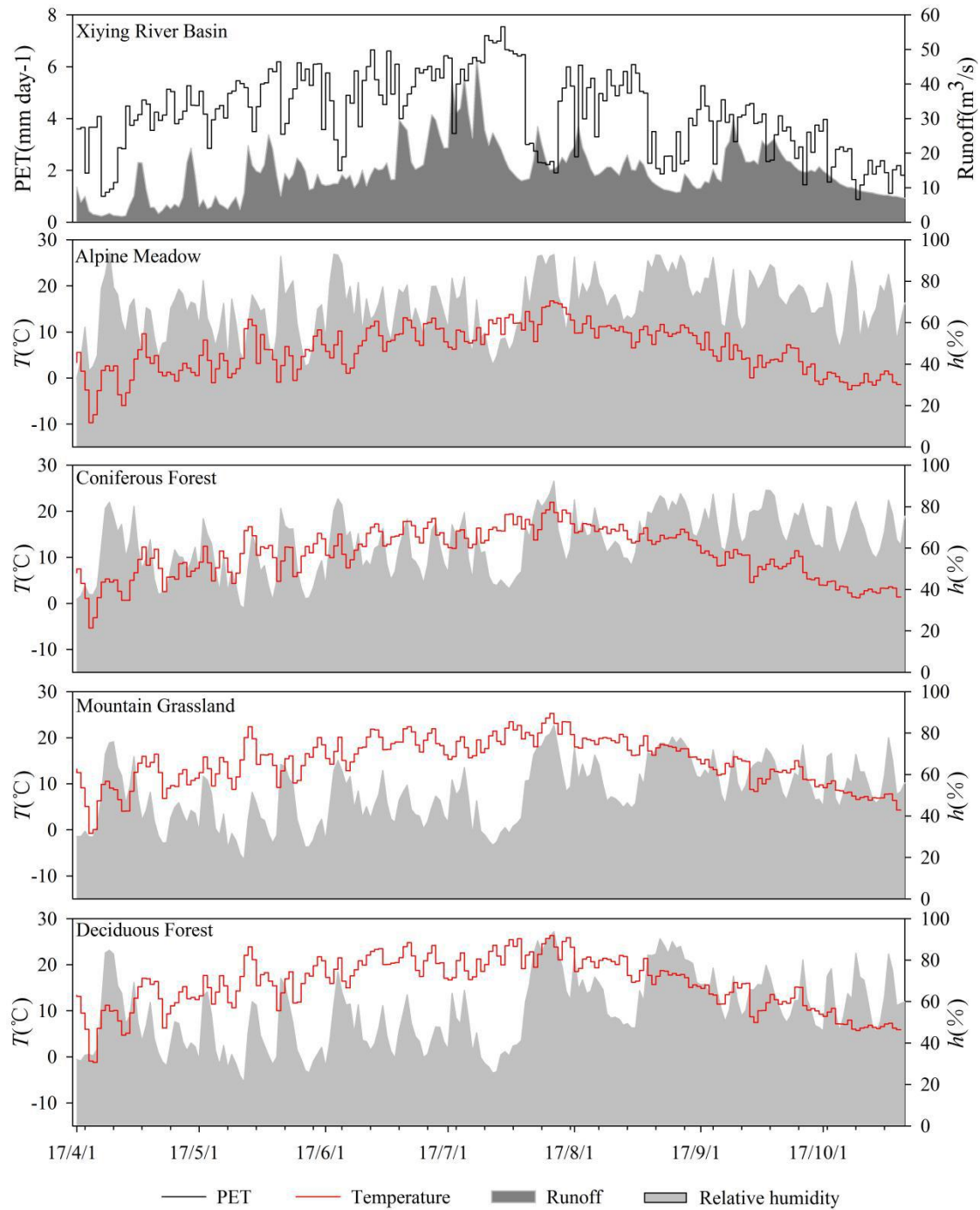
Fig. 2 Climatic and hydrological conditions of Xiying River basin and its vegetation zones

To explore the differences in the natural environment in different vegetation zones, air temperature, atmospheric humidity, and precipitation were used to indicate each research site's temperature and moisture conditions. The hilltop is a typical alpine meadow zone, with a daily average temperature of 6.1°C, ranging from -9.7°C

223 (April 5) to 16.8°C (July 27). The daily average humidity was 68.2%, with little

224 difference in different periods. During the observation period, there were 72

225 precipitation events in the alpine meadow zone, and the total precipitation was 534.3

226 mm, which was relatively evenly distributed each month. In the coniferous forest zone,

227 the daily average temperature during the study period was 10.9°C, ranging from

228 -5.4°C (April 5) to 22.0°C (July 27). The daily average humidity was 62.5%, and the

229 precipitation was 400.6 mm, mainly concentrated from early August to late September.

230 Close to the foothills is the mountain grassland zone, with a daily average temperature

231 of 14.9°C, ranging from -0.7°C (April 5) to 25.3°C (July 27). The average daily

232 humidity was 51.1%, and the precipitation of the vegetation zone during the

233 observation period was 327.2 mm, mainly from late July to mid-August. During the

234 observation period, the daily average temperature in the deciduous forest zone was

235 15.8°C, ranging from -1.2°C (April 6) to 26.3°C (July 27). The daily average

236 humidity was 54.7%, and the total precipitation was 250.6 mm, which was

237 concentrated in the month from late July to late August. The temperatures of the

238 studied regions were ordered as follows: AM (alpine meadow) < CF (coniferous

239 forest) < MG (mountain grassland) < DF (deciduous forest). The humidities of the

240 studied regions were ordered as follows: AM > CF > MG > DF (Fig. 2).

241 **4.2 Temporal variation in water stable isotopes in different vegetation zones**

242 Influenced by different water sources and complex weather conditions in the

243 precipitation process, the isotopic compositions of precipitation in the four vegetation

244 zones were different during the study period. The mean values of δ^2H and δ^{18}O in the

245 alpine meadow zone (number of samples: 72) were -73.1‰±36.3‰ (-163.9~13.7‰)

246 and -10.0‰±4.3‰ (-23.1~-1.3‰), respectively. The average δ^2H and δ^{18}O values of

247 the coniferous forest zone (number of samples: 42) were -42.0‰±37.2‰

248 (-117.8~13.0‰) and -7.1‰±4.7‰ (-17.4~-0.1‰), respectively. The average δ^2H and

249 δ^{18}O values of the mountain grassland zone (number of samples: 37) were

250 -37.4‰±30.5‰ (-103.1~4.2‰) and -5.9‰±3.9‰ (-15.1~-0.9‰), respectively. The

251 average δ^2H and δ^{18}O values of the deciduous forest zone (number of samples: 40)

252 were -31.8‰±42.8‰ (-110.2~23.2‰) and -5.8‰±5.5‰ (-15.2~3.2‰), respectively

253 (Table 2). The maximum isotopic values of the four vegetation zones appeared on

254 August 4 (AM: 13.7‰, δ^2H; -1.3‰, δ^{18}O), August 10 (CF: 13.0‰, δ^2H; -0.1‰,

255 δ^{18}O), August 7 (MG: 4.2‰, δ^2H; -0.9‰, δ^{18}O) and August 13 (DF: 23.2‰, δ^2H;

256 3.2‰, δ^{18}O). The highest temperature in each vegetation zone appeared on July 27.

257 The high temperature caused the precipitation to undergo strong below-cloud

258 evaporation during the fall, leading to the enrichment of isotopes. In addition, the

259 atmospheric precipitation isotopes of the four vegetation zones had similar temporal

260 variations: from April to August, the fluctuations in δ^2H and δ^{18}O increased, reached

261 the maximum in mid-August, and then gradually decreased (Fig. 3).

262 **Table 2** General characteristics of precipitation δ^2H and δ^{18}O in different vegetation areas

263 from April to October 2017

Vegetation zone	δ^2H/‰				δ^{18}O/‰			
	Max	Min	mean	SD	Max	Min	mean	SD
AM	13.7	-163.9	-73.1	36.3	-1.3	-23.1	-10.0	4.3
CF	13.0	-117.8	-42.0	37.2	-0.1	-17.4	-7.1	4.7
MG	4.2	-103.1	-37.4	30.5	-0.9	-15.1	-5.9	3.9
DF	23.2	-110.2	-31.8	42.8	3.2	-15.2	-5.8	5.5

264
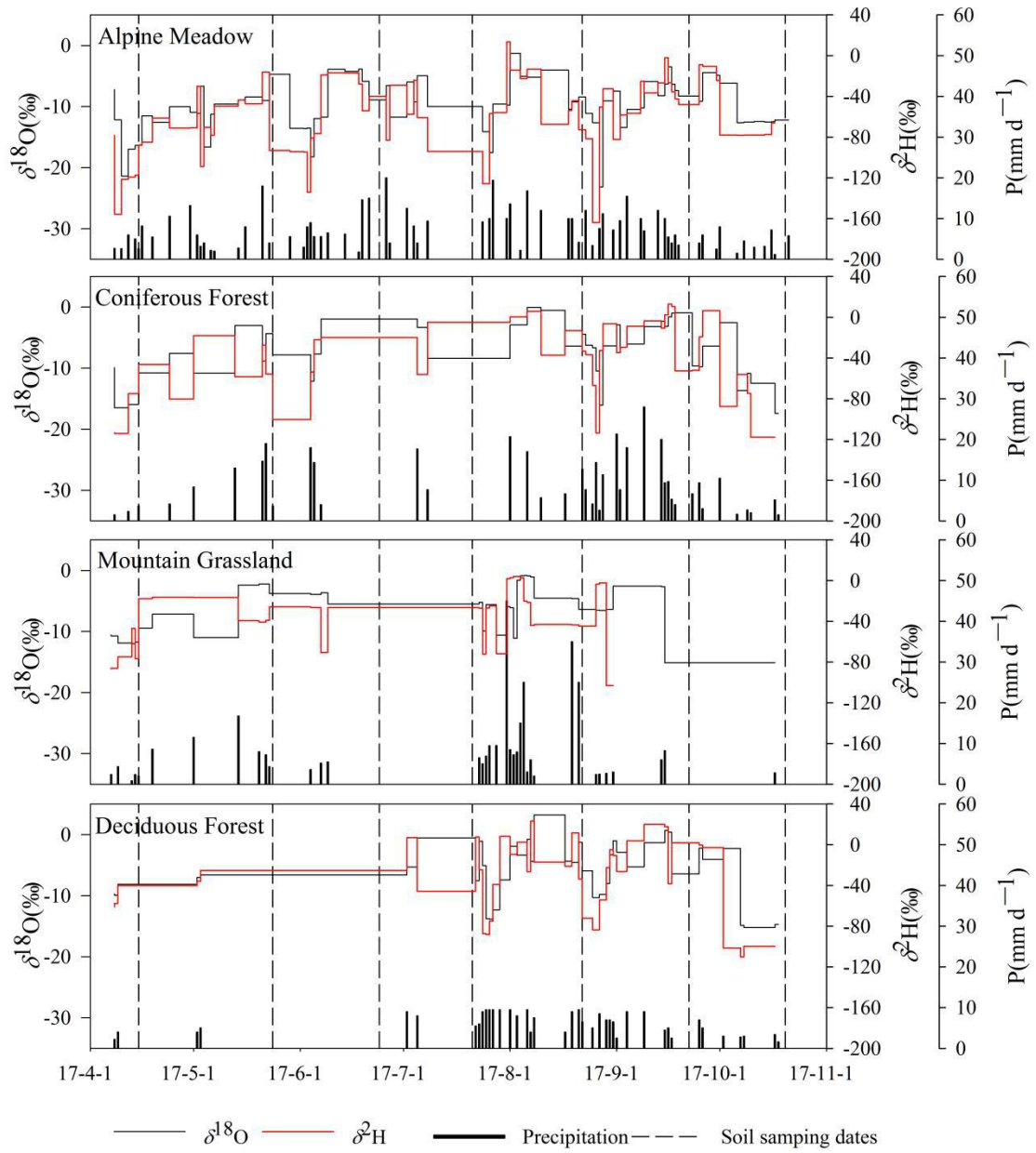
Fig. 3 Time series of rainfall and isotope characteristics in different vegetation zones in Xiying River Basin, with dotted lines indicating the date of soil water sampling

The monthly variation in soil water isotopes records the signal of precipitation input and evaporation. The low-temperature environment and abundant precipitation events in the alpine meadow make the monthly average δ^2H and $\delta^{18}O$ of soil water more depleted than other vegetation zones (-69.4~-51.6‰, δ^2H; -7.5~-10.3‰, δ^2H). Despite this, the SWlc-excess of most samples at this station was still negative, and there were different degrees of evaporation in the process of precipitation penetrating

the soil and mixing with original pore water, among which evaporation fractionation was stronger in July (-11.9‰ lc-excess) and October (-14.5‰ lc-excess). The soil water isotopes of the coniferous forest gradually changed seasonally. From April to July, precipitation was scarce, the temperature rose, and the isotopes of soil water were gradually enriched on the surface (-52.7~-29.5‰, δ^2H; -7.0~-2.1‰, δ^2H), reaching the peak value of the observation period in July (-29.5‰, δ^2H; -2.1‰, $\delta^{18}O$), and continuous rainfall input from late July to mid-August resulted in soil water isotope depletion (-57.0‰, δ^2H; -8.1‰, $\delta^{18}O$). SWlc-excess was an obvious fractionation signal opposite to the trend of isotope change, reaching the lowest value (-26.3‰) in the sampling period in July, and the change in air temperature and precipitation controlled the evaporation intensity. From April to July, the isotopic value of surface soil water in the mountain grassland was higher ($\delta^{18}O$ was greater than zero), and SWlc-excess was lower than -30‰. During this period, the evaporation and fractionation of shallow soil water were intense. Similar to in the coniferous forest, in the mountain grassland, the input of heavy precipitation from late July to mid-August led to the depletion of soil water isotopes. There was only sporadic rainfall in the deciduous forest from April to July, and the soil water isotopes were gradually enriched on the surface (-46.1~-18.2‰, δ^2H; -4.7~0.2‰, δ^2H), reached a peak in June when there was no rainfall event (-18.2‰, δ^2H; 0.2‰, $\delta^{18}O$), and then became depleted (-53.2‰, δ^2H; -5.2‰, $\delta^{18}O$). In addition, due to the influence of the Xiying Reservoir and vegetation coverage, the isotopic enrichment degree of soil water in this vegetation zone was lower than that in the mountain grassland. As the most intuitive form of water change, the gravimetric water content was always at a low value in July (AM: 21.0%; CF: 14.8%; MG: 11.9%; DF: 14.9%), when the evaporation was the strongest, and it was most obvious in shallow soil (Table 3) (Fig. 4).

Table 3 General characteristics of soil water δ^2H, δ^{18}O, lc-excess and GWC in different

vegetation areas from April to October 2017

Month	Vegetation zone	δ^2H/‰			δ^{18}O/‰			lc-excess/‰			GWC/%		
		Max	Min	Mean	Max	Min	Mean	Max	Min	Mean	Max	Min	Mean
4	AM	-55.2	-70.7	-65.6	-8.5	-10.8	-10.1	-2.7	-7.1	-4.7	25.9	23.0.0.	24.7
	CF	-52.7	-72.2	-63.9	-7.0	-9.9	-8.9	-4.0	-12.0	-8.4	27.6	14.9	20.0
	MG	-7.32	-50.6	-41.0	2.8	-5.8	-3.9	-8.8	-36.8	-19.4	21.7	6.5	14.7
	DF	-46.1	-69.4	-62.1	-4.7	-9.9	-8.5	-2.5	-23.2	-9.7	27.7	19.4	21.8
5	AM	-46.1	-76.5	-66.4	-7.4	-12.2	-10.1	-2.6	-7.7	-4.9	32.6	23.2	28.9
	CF	-45.8	-61.9	-53.5	-5.3	-8.4	-7.0	-9.3	-17.7	-13.0	22.6	9.0	16.1
	MG	-6.7	-47.3	-39.2	2.9	-6.5	-4.3	-4.5	-36.2	-14.4	15.7	7.6	11.2
	DF	-30.8	-63.5	-53.8	-1.9	-9.4	-6.9	-3.2	-30.1	-13.6	26.0	11.7	17.7
6	AM	-62.5	-83.9	-69.4	-8.9	-12.6	-10.3	-1.5	-8.4	-5.8	33.3	21.9	26.0
	CF	-45.8	-78.4	-58.7	-5.1	-12.0	-7.8	5.5	-26.6	-8.5	32.1	10.0	21.3
	MG	-19.7	-74.9	-46.9	0.8	-11.8	-5.8	13.0	-33.7	-11.0	19.3	7.5	14.2
	DF	-18.2	-64.9	-51.7	0.2	-9.0	-5.9	-4.6	-38.2	-19.4	13.5	8.4	11.1
7	AM	-47.3	-60.1	-51.6	-6.9	-8.4	-7.5	-8.8	-14.8	-11.9	25.4	19.0	21.0
	CF	-29.5	-51.4	-41.6	-2.1	-7.9	-5.6	-2.6	-26.3	-11.2	24.3	7.2	14.8
	MG	-10.6	-48.4	-39.2	2.3	-6.4	-4.1	-5.8	-35.8	-16.1	18.7	6.3	11.9
	DF	-35.1	-69.0	-54.1	-1.7	-8.7	-5.5	-14.8	-35.3	-24.5	18.2	11.8	14.4
8	AM	-58.5	-80.3	-66.6	-8.4	-11.6	-9.6	-6.1	-15.4	-9.7	28.1	19.5	25.1
	CF	-57.0	-75.5	-66.4	-8.1	-9.8	-9.2	-2.5	-13.1	-8.3	21.4	8.7	16.3
	MG	-34.2	-53.8	-44.0	-3.2	-5.5	-4.4	-14.7	-22.6	-18.7	11.3	9.5	10.4
	DF	-53.2	-84.3	-67.6	-5.2	-13.5	-9.2	6.8	-26.1	-9.6	23.6	14.7	20.6
9	AM	-48.0	-79.2	-61.0	-7.8	-11.1	-9.2	-4.3	-10.4	-7.2	29.9	20.3	25.3
	CF	-52.5	-67.7	-60.7	-7.8	-10.1	-8.8	-0.1	-11.3	-6.0	31.3	9.3	20.5
	MG	-32.3	-45.3	-38.8	-3.5	-4.4	-4.0	-9.1	-23.8	-16.5	15.3	9.1	13.0
	DF	-30.5	-77.0	-59.8	-3.1	-11.4	-8.2	-1.8	-19.3	-9.3	25.8	14.7	19.1
10	AM	-42.4	-73.5	-58.9	-6.1	-9.8	-7.9	-12.2	-18.2	-14.5	36.2	25.4	29.5
	CF	-59.1	-66.3	-61.7	-8.8	-10.5	-9.5	5.1	-5.3	-1.5	30.0	16.8	23.1
	MG	-50.3	-66.7	-58.3	-5.6	-8.3	-7.1	-5.5	-18.4	-11.9	18.3	11.4	15.8
	DF	-38.0	-61.8	-48.3	-2.7	-8.2	-4.9	-11.9	-34.8	-23.9	25.5	8.9	17.2

305
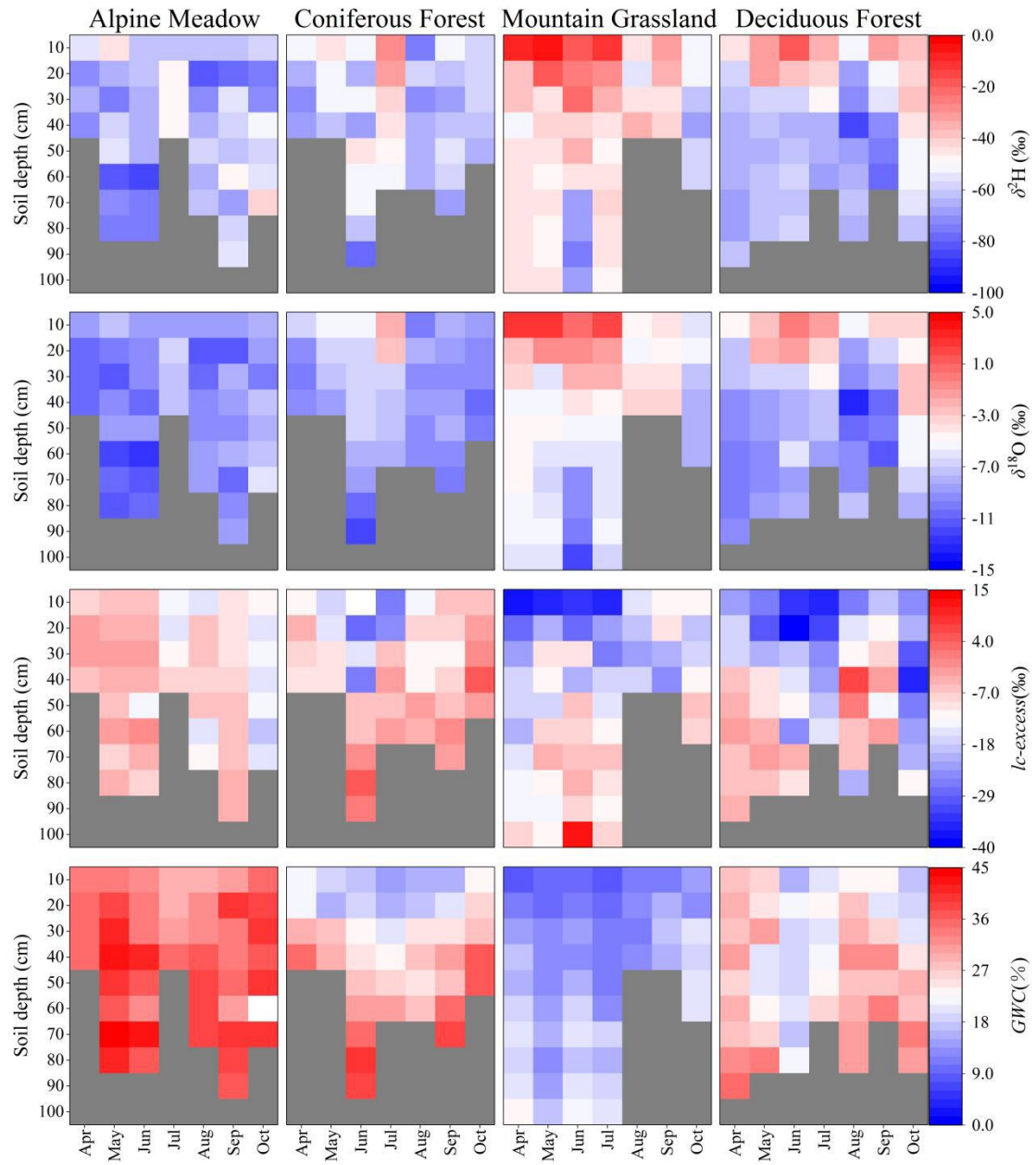
Fig. 4 Heat map of the soil depth profile of δ²H, δ¹⁸O, lc-excess and GWC in

different vegetation zones, and the layer lacking measurement is indicated by the

grey color

4.3 Spatial variation in water stable isotopes in different vegetation zones

Isotope data of precipitation and soil water obtained from different vegetation

zones are shown in dual-isotope space in Fig. 5. At the alpine meadow observation

station, the slope (8.4) and intercept (23) of the LMWL were higher than those of the

GMWL. The slope of the LMWL in the other three vegetation zones was lower than

that of the GMWL and gradually decreased with decreasing altitude. With the

315 decrease in altitude, the slope of the SWL in all vegetation zones except for the

316 deciduous forest SWL decreased (AM: 6.4; CF: 4.7; MG: 3.4; DF: 4.1), indicating

317 that the evaporation of soil moisture increased. On the one hand, the vegetation

318 coverage of the deciduous forest site was higher. On the other hand, the Xiying

319 Reservoir enhanced the regional air humidity and decreased the local water vapor

320 circulation driving force.

321
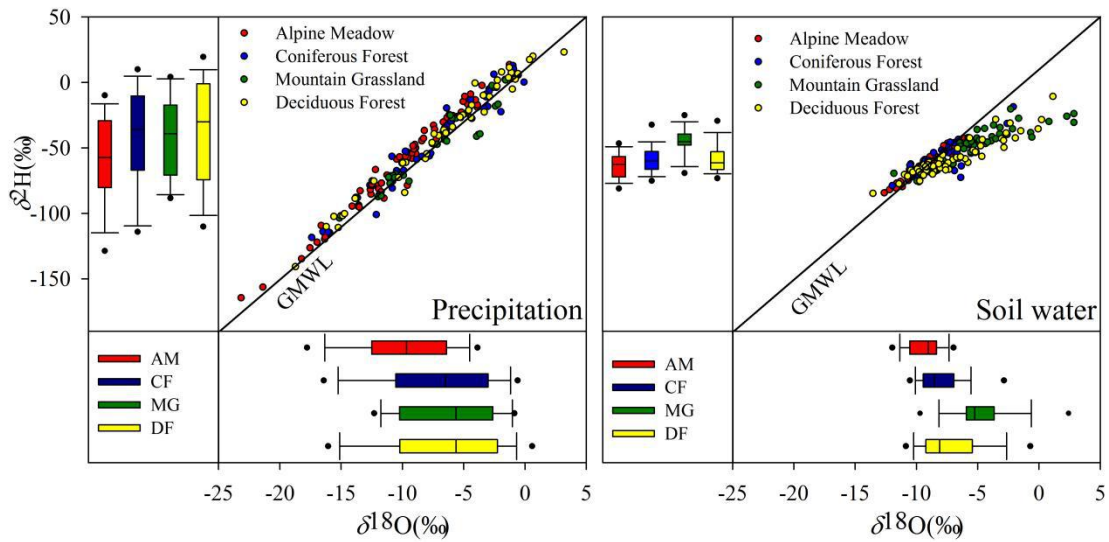
Fig. 5 Dual-isotope space of precipitation (left) and soil water (right) isotope data of

four vegetation zones. In the box plots, the box represents the 25%-75% percentile,

the line in the box represents the median (50th percentile), the required line

indicates 90th and 10th percentile, and the point indicates the 95th and 5th

percentile.

327 During the study period, compared with that in other vegetation belts, the surface

328 isotopic value of the soil water in the mountain grassland was relatively enriched

329 (-24.3‰, δ^2H; -0.8‰, δ^{18}O), the lc-excess was smaller and deeper into the middle

330 and lower soil layers (-25.8‰), and the gravimetric water content was relatively low

331 (8.4%). Due to the difference in vegetation types and the influence of reservoirs, this

332 change did not have an obvious elevation effect. Although the elevation was low, the

333 soil water of the deciduous forest had more depleted isotopic characteristics and

334 higher soil moisture than those of the mountain grassland in most samples. Soil

335 profiles obtained from different vegetation zones can reflect the evaporation signals of

water. The low-temperature natural environment made alpine meadow soil less affected by evaporation (lc-excess > -20‰), and the gravimetric water content was high (gravimetric water content > 20%) during the whole study period. The surface soil water of the coniferous forest was easily affected by climate and had a higher isotopic composition (-29.5‰, $\delta^2 H$; -2.1‰, $\delta^{18} O$) and lower lc-excess (-26.3‰). Due to evaporation, soil water isotopes in the mountain grassland and deciduous forest areas were enriched in the surface soil layer. In particular, in the mountain grassland, the average values of $\delta^2 H$ and $\delta^{18} O$ in the 0-10 cm soil layer were as high as -24.4‰ and -1.2‰, respectively, and SWlc-excess was lower than -25‰, even close to -40‰ in some samples. In this case, the evaporation signals can easily penetrate the deep soil, making the gravimetric water content values at all the sampling sites lower than 20% (Fig. 4; Fig. 6).
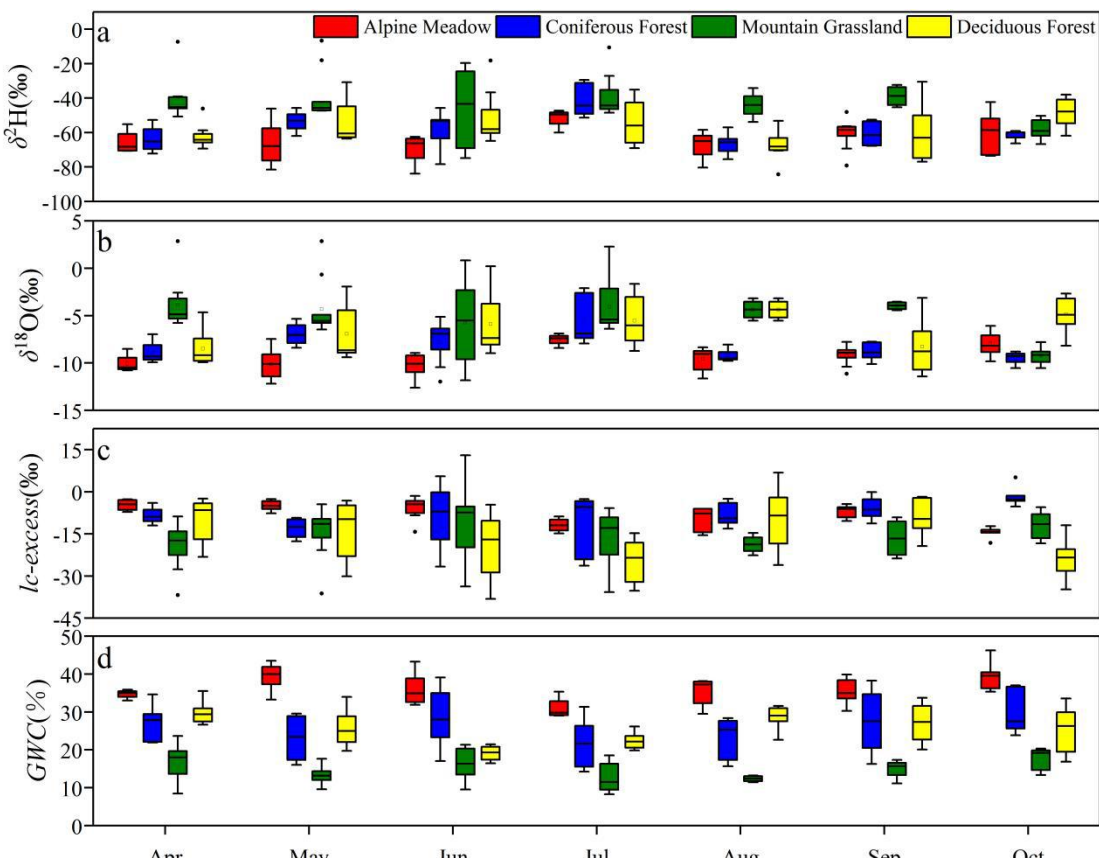
Fig. 6 The variation of $\delta^2 H$, $\delta^{18} O$, lc-excess and GWC in different vegetation zones in each sampling

4.4 Variations in the water storage capacity of the 0-40 cm soil layer in different vegetation areas

This study used soil water to calculate the water storage of the 0-40 cm soil layer in the four vegetation zones during the observation period (Fig 7). The water storage capacity of the alpine meadow gradually decreased from April to July (209.7~167.2 mm), and the water storage capacity increased after July (167.2~201.8 mm). The monthly average water storage capacity was the lowest at 0-10 cm (43.0 mm) and the highest at 30-40 cm (51.7 mm). The water storage capacity of the coniferous forest gradually decreased from April to July (150.1~101.2 mm), and the water storage capacity increased after July (101.2~160.0 mm). The monthly average water storage capacity was the lowest at 0-10 cm (28.0 mm) and the highest at 30-40 cm (40.0 mm). The water storage capacity of the mountain grassland gradually decreased from April to July (80.3~64.0 mm), and the water storage capacity increased after July (64.0~104.6 mm). The monthly average water storage capacity was the lowest at 0-10 cm (17.5 mm) and the highest at 20-30 cm (22.0 mm). The water storage capacity of the deciduous forest gradually decreased from April to June (159.3~104.0 mm), the water storage capacity increased from June to August (104.0~154.0 mm), and there was a decrease from August to October (154.0~111.8 mm). The monthly average water storage capacity was the lowest at 0-10 cm (29.1 mm) and the highest at 20-30 cm (35.0 mm). In general, the soil water storage capacity of the 0-10 cm soil layer was less than that of the other soil layers. The order of the water storage capacity of the 0-40 cm soil layer in the four vegetation zones is alpine meadow (46.9 mm) > deciduous forest (33.0 mm) > coniferous forest (32.1 mm) > mountain grassland (20.3 mm).

375
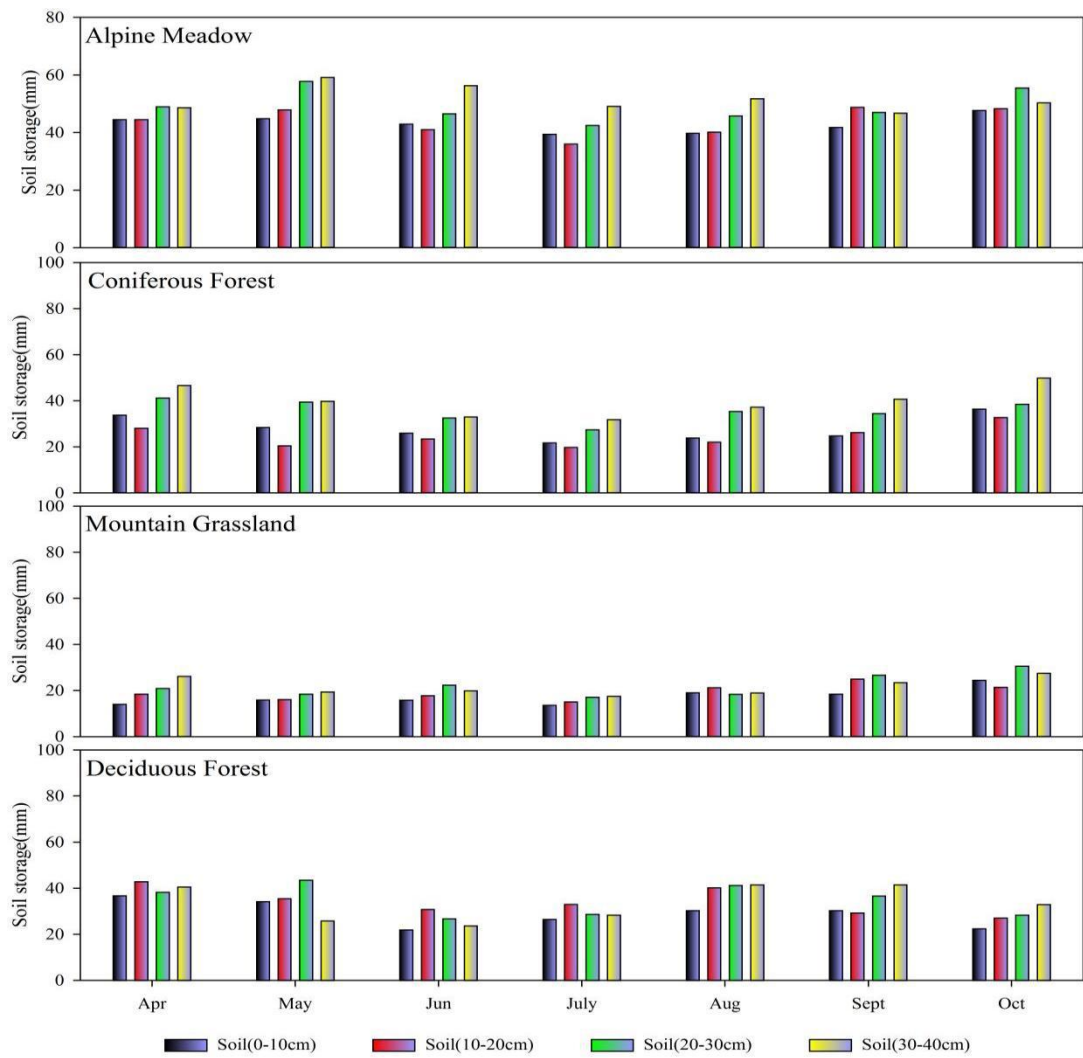
Fig. 7 Monthly variation of soil water storage in 0-40cm soil layer of different

vegetation zones

5. Discussion

5.1 Evaporation of soil moisture in different vegetation zones

In the arid river source area, the replenishment of soil moisture mainly comes from precipitation. The slope of the regional atmospheric precipitation line can reflect the strength of local evaporation. Due to a low atmospheric temperature, low cloud base height, and low air-saturated water vapor loss, the alpine meadow zone was weakly affected by secondary evaporation during precipitation. There, the slope of the LMWL (8.4) was even higher than that of the GMWL (Hughes and Crawford, 2012). As the altitude decreased, the secondary evaporation under clouds strengthened, and

387 the slope of the LMWL of each vegetation zone decreased (Pang et al., 2011). The

388 slope of SWL can indicate the strength of soil moisture evaporation in each vegetation

389 zone, the evaporation intensity results of the four vegetation zones followed the order

390 of mountain grassland (SWL$_{slop}$: 3.4) > deciduous forest (SWL$_{slop}$: 4.1) > coniferous

391 forest (SWL$_{slop}$: 4.7) > alpine meadow (SWL$_{slop}$: 6.4) (Fig 5). The dynamic changes in

392 lc-excess of soil profiles in different vegetation areas reflect the process of soil water

393 evaporation caused by drought during the study period. The monthly average value of

394 SWlc-excess in the alpine meadow zone was less than 0, and the minimum value was

395 -11.9‰ (July). Although the vegetation belt was subject to different degrees of

396 evaporation each month, it was less affected by drought, and it was difficult for

397 evaporation to penetrate into the middle and lower soil layers. The SWlc-excess of the

398 coniferous forest belt was greater than that of the alpine meadow from April to June.

399 The evaporation was the strongest in July (-11.2‰ lc-excess). Similar to in the alpine

400 meadow, in the coniferous forest belt, evaporation mainly occurred in the topsoil. The

401 vegetation coverage of the mountain grassland zone was low, and the arid

402 environment made the isotopes of the surface soil produce strong evaporation signals

403 (lc-excess was close to -40‰). In most samples, the SWlc-excess of the 60-80 cm soil

404 layer was negative. The evaporation signal shifted to the lower layer of the soil

405 (Barnes and Allison, 1988; Zimmermann et al., 1966). Similar evaporation signals

406 have been found in the Mediterranean and arid climate regions (McCutcheon et al.,

407 2017; Sprenger et al., 2016). Evaporation signals exist in only the surface soil in

408 humid areas, and there is no difference between lc-excess and 0 in the soil layer below

409 20 cm (Sprenger et al., 2017). The monthly surface soil evaporation of deciduous

410 forest was less than that of mountain grassland from April to June, and it was greater

411 than that of mountain grassland after July, mainly due to the influence of the

412 vegetation and reservoirs. There were commonalities in the soil moisture changes in

413 different vegetation zones characterized by more enriched isotopes, stronger

414 evaporation signals, and lower moisture content in the shallow soil. With increasing

415 soil depth, the isotope gradually became depleted, and the evaporation signal was

416 gradually weakened until it disappeared. The evolution of the investigated isotopes,

lc-excess, and gravimetric water content in the unsaturated soil showed differences among different vegetation zones. From a high altitude to a low altitude, the isotopic value of the surface gradually increased, and the evaporation signal increased (Fig 4; Fig 6).

5.2 Memory effects of precipitation input, mixing and rewetting

The changes in soil water isotopes and soil moisture can evaluate the input, mixing, and rewetting precipitation process in different vegetation areas. The main methods of precipitation input are plug flow and preferential flow. Plug flow is the complete mixing of water through the soil matrix with shallow free water. Under the action of plug flow, precipitation infiltrates along the hydraulic gradient, pushing the original soil water downward. Preferential flow means that precipitation uses soil macropores to quickly penetrate shallow soil to form deep leakage (Tang and Feng, 2001). After precipitation, the variability of isotope signals at a certain soil depth can identify the seepage method of water (Peralta-Tapia et al., 2015). During the study period, the soils of the alpine meadow and coniferous forest areas were seasonally frozen and thawed year-round, and the difference in the soil isotope profile was small. The soil moisture profile showed a trend of water increasing from top to bottom, indicating the influence of the previous precipitation. The soil was humid, so the replenishment of soil water by precipitation had the characteristics of top-down piston replenishment. Preferential infiltration showed high variability in isotopic signals (Brodersen et al., 2000), and the rainwater in mountain grassland and deciduous forest flowed into the deep soil rapidly through the soil matrix via exposed soil fissures and roots. This resulted in the sudden depletion of soil isotopes at a depth of 60-100 cm. This may be due to the more recent depleted precipitation that quickly reached this depth and the preferential infiltration into the soil. Water movement and mixing in the unsaturated zone can be observed in the spatiotemporal variation in isotopes within 1 m of the soil profile, and the alpine meadow and coniferous forest zones underwent considerable rainfall. After a short period of weak evaporation, the soil was rewetted by the next rainfall. In the alpine meadow, the soil moisture remained above 20% each month. The mountain grassland and deciduous forest zones had only sporadic

447   precipitation from mid-May to late July, and the soil moisture evaporated rapidly.

448   With the decrease in air temperature and the occurrence of continuous precipitation

449   after July, the soil was rewetted after two months of drought, and both vegetation

450   zones showed the replacement and mixing of soil water isotopes and precipitation.

451   The results showed that the soil water storage capacity of the alpine grassland was

452   seriously insufficient, reflecting the incomplete rewetting of the soil by precipitation

453   at the end of the study. In addition, low soil water storage capacity will enrich the

454   remaining soil water isotopes (Barnes and Allison, 1988; Zimmermann et al., 1966).

455   We observed the memory effect of soil rewetting caused by precipitation input and the

456   mixing of different vegetation areas during the entire study period. The changes in

457   soil moisture in each vegetation area reflect different climatic and hydrological

458   characteristics (Fig. 4; Fig. 6).

459   **5.3 Influencing factors of soil water storage capacity in arid headwater areas**

460   As the temperature decreased rapidly with increasing height, precipitation and

461   humidity increased to a certain extent, and the vegetation showed a strip-like

462   alternation approximately parallel to the contour line, forming zonal vegetation with

463   obvious differentiation (Yin et al., 2020). The dry-wet conditions of different

464   vegetation zones restricted the soil water storage capacity in the basin. In the process

465   of low-altitude vegetation zone replacement, the precipitation decreased, the

466   temperature rose, the groundwater level dropped, and the soil water storage capacity

467   was weak (Coussement et al., 2018; Kleine et al., 2020). The soil water storage

468   capacity of the alpine meadow zone with low-temperature and rainy weather was

469   higher than that of other vegetation zones (results of the 0-40 cm soil layers from

470   April to October: AM: 187.8 mm; CF: 128.4 mm; MG: 81.2 mm; DF: 132.1 mm).

471   During the study period, the soil water storage capacity (0-40 cm) exceeded 165 mm

472   each month. With the decrease in altitude, the monthly difference in dry-wet

473   conditions in each vegetation zone gradually became obvious. With the increase in

474   temperature in summer, the environment became dry, and the soil water storage

475   capacity weakened (Sprenger et al., 2017). The soil water storage capacity of the

476   coniferous forest zone began to decrease in April, and the water storage capacity of

the 0-40 cm layer reached the minimum value (101.2 mm) in July. The variation in temperature and precipitation was the main reason for the monthly difference (Dubber and Werner, 2019). Although there was a certain water storage capacity in the coniferous forest with some transpiration loss, the soil water storage capacity in this vegetation zone was not strong. The water storage capacity of mountain grassland soil was lower than that of other vegetation zones. The continuous dry and warm weather in spring and summer led to the water storage capacity of 0-40 cm soil being lower than that of 100 mm every month. In particular, drought stress leads to insufficient soil moisture, making it difficult to maintain plant demand, resulting in sparse vegetation and large-scale exposed surface soil, which further accelerates surface water loss. The continuous precipitation from the end of July prevented further drought development, and the water input gradually restored the soil water storage capacity (Kleine et al., 2020). The deciduous forest had hydrothermal conditions similar to those of the mountain grassland, but the soil porosity of the forest zone was obviously larger than that of the barren land, and its permeability was higher than that of the barren land. Precipitation infiltrated the ground through roots and turned into groundwater. The forest acted as a reservoir due to its strong water storage and soil conservation capacity (Sprenger et al., 2019). The water storage capacity of the 0-40 cm soil layer in the deciduous forest was higher than 100 mm at each sampling time. In addition, the water content of the 0-40 cm soil layer in each vegetation zone increased with the deepening of the soil layer, and the water storage capacity of the surface soil was weak. The difference in soil properties also led to more water storage in the middle and lower soil layers with higher clay contents (Milly, 1994) (Fig. 7). Climate warming and the spatiotemporal imbalance of water resources have disturbed the ecological-water balance of different vegetation zones in inland river source areas (Liu et al., 2015). Plant growth mainly depends on the water stored in shallow soil layers (Amin et al., 2020). Drought reduces soil water storage and inhibits plant growth (Li et al., 2020). To effectively improve and manage water resources in arid water source areas, exploring the heterogeneity of hydrological

506 processes among different vegetation zones is necessary. This will provide a reference
507 for the formulation of ecological policies.

6. Conclusion

509 This work provides further insights into the movement and mixing of soil water in
510 different vegetation zones in arid source regions. During the study period, the
511 dynamic changes in lc-excess in the soil profiles of different vegetation zones
512 reflected the evaporation signals caused by drought. Soil water evaporation in spring
513 and summer and insufficient precipitation during the drought period were the main
514 driving forces of isotopic enrichment in the surface soil. The soil water evaporation
515 intensity results of the four vegetation zones followed the order of mountain grassland
516 (SWL$_{slop}$: 3.4) > deciduous forest (SWL$_{slop}$: 4.1) > coniferous forest (SWL$_{slop}$: 4.7) >
517 alpine meadow (SWL$_{slop}$: 6.4). In the mountain grassland and deciduous forest zones,
518 drought caused the evaporation signal to penetrate deep into the middle and lower soil
519 layers. The SWlc-excess below 70 cm of the ground surface remained negative. Soil
520 water isotopes and gravimetric water content record the process of soil rewetting
521 caused by precipitation input and mixing. The alpine meadow and coniferous forest
522 zones were enriched in precipitation. After a short period of weak evaporation, the
523 soil was rewetted by the next precipitation event. There was only sporadic
524 precipitation in the mountain grassland and deciduous forest belt from mid-May to
525 late July. After July, the temperature dropped, and continuous precipitation wet the
526 soil again after two months of drought. The mountain grassland and deciduous forest
527 zones had only sporadic precipitation from mid-May to late July. With the decrease in
528 air temperature and continuous precipitation after July, the soil was rewetted after two
529 months of drought. Moisture and temperature conditions were the key factors that
530 restricted the soil water storage capacity in the different vegetation zones. The water
531 storage capacity of the 0-40 cm soil layer results followed the order of alpine meadow
532 (46.9 mm) > deciduous forest (33.0 mm) > coniferous forest (32.1 mm) > mountain
533 grassland (20.3 mm). The water storage capacity of the surface soil in each vegetation
534 zone was weak, and more water was stored in the middle and lower soil layers with

higher clay contents. The research results can be applied to arid and semi-arid alpine regions and have reference significance for latitude and longitude differentiation. This study mainly emphasized the Spatio-temporal heterogeneity of soil water evaporation, infiltration, and water storage in different vegetation zones. These results are of great value for understanding regional hydrological processes and ecological restoration services in environmentally fragile areas. Furthermore, we hope this study can be used as a basic statement because we continue to use stable water isotopes as a data source to understand hydrological processes from the perspective of process mechanisms.

References

Allen, R. G.: Crop evapotranspiration :guidelines for computing crop water requirements, FAO irrigation and drainage paper, edited, Food and Agriculture Organization of the United Nations, Rome, 300 pp., 1998.

Amin, A., Zuecco, G., Geris, J., Schwendenmann, L., McDonnell, J. J., Borga, M., and Penna, D.: Depth distribution of soil water sourced by plants at the global scale: A new direct inference approach, Ecohydrology, 13, e2177, https://doi.org/10.1002/eco.2177, 2020.

Barnes, C. J., and Allison, G. B.: Tracing of water movement in the unsaturated zone using stable isotopes of hydrogen and oxygen, J. Hydrol., 100, 143-176, https://doi.org/10.1016/0022-1694(88)90184-9, 1988.

Brodersen, C., Pohl, S., Lindenlaub, M., Leibundgut, C., and Wilpert, K. V.: Influence of vegetation structure on isotope content of throughfall and soil water, Hydrol. Process., 14, 1439-1448,
https://doi.org/10.1002/1099-1085(20000615)14:8<1439::AID-HYP985>3.0.CO;2-3, 2000.

Brooks, R. J., Barnard, H. R., Coulombe, R., and McDonnell, J. J.: Ecohydrologic separation of water between trees and streams in a Mediterranean climate, Nat. Geosci., 3, 100-104, https://doi.org/10.1038/ngeo722, 2010.

Coussement, T., Maloteau, S., Pardon, P., Artru, S., Ridley, S., Javaux, M., and Garré, S.: A tree-bordered field as a surrogate for agroforestry in temperate regions: Where does the water go? Agr. Water Manage., 210, 198-207, https://doi.org/10.1016/j.agwat.2018.06.033, 2018.

Dansgaard, W.: Stable isotopes in precipitation, Tellus, 16, 436-468, https://doi.org/10.3402/tellusa.v16i4.8993, 1964.

Dubbert, M., and Werner, C.: Water fluxes mediated by vegetation: emerging isotopic insights at the soil and atmosphere interfaces, New Phytologist, 221, 1754-1763, https://doi.org/10.1111/nph.15547, 2019.

Duvert, C., Stewart, M. K., Cendón, D. I., and Raiber, M.: Time series of tritium, stable isotopes and chloride reveal short-term variations in groundwater contribution to a stream, Hydrol. Earth Syst. Sci., 20, 257-277, https://doi.org/10.5194/hess-20-257-2016, 2016.

Ferretti, D. F., Pendall, E., Morgan, J. A., Nelson, J. A., LeCain, D., and Mosier, A. R.: Partitioning evapotranspiration fluxes from a Colorado grassland using stable isotopes: Seasonal variations and ecosystem implications of elevated atmospheric CO2, Plant Soil, 254,

291-303, https://doi.org/10.1023/A:1025511618571, 2003.

Gibson, J. J., Holmes, T., Stadnyk, T. A., Birks, S. J., Eby, P., and Pietroniro, A.: Isotopic constraints on water balance and evapotranspiration partitioning in gauged watersheds across Canada, Journal of Hydrology: Regional Studies, 37, 100878, https://doi.org/10.1016/j.ejrh.2021.100878, 2021.

Grant, G. E., and Dietrich, W. E.: The frontier beneath our feet, Water Resour. Res., 53, 2605-2609, https://doi.org/10.1002/2017WR020835, 2017.

Hughes, C. E., and Crawford, J.: A new precipitation weighted method for determining the meteoric water line for hydrological applications demonstrated using Australian and global GNIP data, J. Hydrol., 464-465, 344-351, https://doi.org/10.1016/j.jhydrol.2012.07.029, 2012.

Kleine, L., Tetzlaff, D., Smith, A., Wang, H., and Soulsby, C.: Using water stable isotopes to understand evaporation, moisture stress, and re-wetting in catchment forest and grassland soils of the summer drought of 2018, Hydrol. Earth Syst. Sci., 24, 3737-3752, https://doi.org/10.5194/hess-24-3737-2020, 2020.

Koeniger, P., Gaj, M., Beyer, M., and Himmelsbach, T.: Review on soil water isotope-based groundwater recharge estimations, Hydrol. Process., 30, 2817-2834, https://doi.org/10.1002/hyp.10775, 2016.

Landwehr, J. M., and Coplen, T. B.: Line-conditioned excess: a new method for characterizing stable hydrogen and oxygen isotope ratios in hydrologic systems, International conference on isotopes in environmental studies, 2006, 132-135, 2006.

Landwehr, J. M., Coplen, T. B., and Stewart, D. W.: Spatial, seasonal, and source variability in the stable oxygen and hydrogen isotopic composition of tap waters throughout the USA, Hydrol. Process., 28, 5382-5422, https://doi.org/10.1002/hyp.10004, 2014.

Li, X., Piao, S., Wang, K., Wang, X., Wang, T., Ciais, P., Chen, A., Lian, X., Peng, S., and Peñuelas, J.: Temporal trade-off between gymnosperm resistance and resilience increases forest sensitivity to extreme drought, Nature Ecology & Evolution, 4, 1075-1083, https://doi.org/10.1038/s41559-020-1217-3, 2020.

Liu, Y., Liu, F., Xu, Z., Zhang, J., Wang, L., and An, S.: Variations of soil water isotopes and effective contribution times of precipitation and throughfall to alpine soil water, in Wolong Nature Reserve, China, Catena, 126, 201-208, https://doi.org/10.1016/j.catena.2014.11.008, 2015.

Ma, X., Jia, W., Zhu, G., Ding, D., Pan, H., Xu, X., Guo, H., Zhang, Y., and Yuan, R.: Stable isotope composition of precipitation at different elevations in the monsoon marginal zone, Quatern. Int., 493, 86-95, https://doi.org/10.1016/j.quaint.2018.06.038, 2018.

McCutcheon, R. J., McNamara, J. P., Kohn, M. J., and Evans, S. L.: An evaluation of the ecohydrological separation hypothesis in a semiarid catchment, Hydrol. Process., 31, 783-799, https://doi.org/10.1002/hyp.11052, 2017.

Milly, P. C. D.: Climate, soil water storage, and the average annual water balance, Water Resour. Res., 30, 2143-2156, https://doi.org/10.1029/94WR00586, 1994.

Pang, Z., Kong, Y., Froehlich, K., Huang, T., Yuan, L., Li, Z., and Wang, F.: Processes affecting isotopes in precipitation of an arid region, Tellus B: Chemical and Physical Meteorology, 63, 352-359, https://doi.org/10.1111/j.1600-0889.2011.00532.x, 2011.

Penna, D., Hopp, L., Scandellari, F., Allen, S. T., Benettin, P., Beyer, M., Geris, J., Klaus, J., Marshall, J. D., Schwendenmann, L., Volkmann, T. H. M., von Freyberg, J., Amin, A.,

Ceperley, N., Engel, M., Frentress, J., Giambastiani, Y., McDonnell, J. J., Zuecco, G., Llorens, P., Siegwolf, R. T. W., Dawson, T. E., and Kirchner, J. W.: Ideas and perspectives: Tracing terrestrial ecosystem water fluxes using hydrogen and oxygen stable isotopes – challenges and opportunities from an interdisciplinary perspective, Biogeosciences, 15, 6399-6415, https://doi.org/10.5194/bg-15-6399-2018, 2018.

Penna, D., Stenni, B., Šanda, M., Wrede, S., Bogaard, T. A., Michelini, M., Fischer, B. M. C., Gobbi, A., Mantese, N., Zuecco, G., Borga, M., Bonazza, M., Sobotková, M., Čejková, B., and Wassenaar, L. I.: Technical Note: Evaluation of between-sample memory effects in the analysis of δ^{2}H and δ^{18}O of water samples measured by laser spectroscopes, Hydrol. Earth Syst. Sci., 16, 3925-3933, https://doi.org/10.5194/hess-16-3925-2012, 2012.

Peralta-Tapia, A., Sponseller, R. A., Tetzlaff, D., Soulsby, C., and Laudon, H.: Connecting precipitation inputs and soil flow pathways to stream water in contrasting boreal catchments, Hydrol. Process., 29, 3546-3555, https://doi.org/10.1002/hyp.10300, 2015.

Qu, D., Tian, L., Zhao, H., Yao, P., Xu, B., and Cui, J.: Demonstration of a memory calibration method in water isotope measurement by laser spectroscopy, Rapid Commun. Mass Sp., 34, e8689, https://doi.org/10.1002/rcm.8689, 2020.

Rothfuss, Y., and Javaux, M.: Reviews and syntheses: Isotopic approaches to quantify root water uptake: a review and comparison of methods, Biogeosciences, 14, 2199-2224, https://doi.org/10.5194/bg-14-2199-2017, 2017.

Sharma, H., Ehlers, T. A., Glotzbach, C., Schmid, M., and Tielbörger, K.: Effect of rock uplift and Milankovitch timescale variations in precipitation and vegetation cover on catchment erosion rates, Earth Surf. Dynam., 9, 1045-1072, https://doi.org/10.5194/esurf-9-1045-2021, 2021.

Snelgrove, J. R., Buttle, J. M., Kohn, M. J., and Tetzlaff, D.: Co-evolution of xylem water and soil water stable isotopic composition in a northern mixed forest biome, Hydrol. Earth Syst. Sci., 25, 2169-2186, https://doi.org/10.5194/hess-25-2169-2021, 2021.

Sprenger, M., Leistert, H., Gimbel, K., and Weiler, M.: Illuminating hydrological processes at the soil-vegetation-atmosphere interface with water stable isotopes, Rev. Geophys., 54, 674-704, https://doi.org/10.1002/2015RG000515, 2016.

Sprenger, M., Llorens, P., Cayuela, C., Gallart, F., and Latron, J.: Mechanisms of consistently disjunct soil water pools over (pore) space and time, Hydrol. Earth Syst. Sci., 23, 2751-2762, https://doi.org/10.5194/hess-23-2751-2019, 2019.

Sprenger, M., Tetzlaff, D., and Soulsby, C.: Soil water stable isotopes reveal evaporation dynamics at the soil–plant–atmosphere interface of the critical zone, Hydrol. Earth Syst. Sci., 21, 3839-3858, https://doi.org/10.5194/hess-21-3839-2017, 2017.

Tang, K., and Feng, X.: The effect of soil hydrology on the oxygen and hydrogen isotopic compositions of plants' source water, Earth Planet. Sc. Lett., 185, 355-367, https://doi.org/10.1016/S0012-821X(00)00385-X, 2001.

Tetzlaff, D., Soulsby, C., Buttle, J., Capell, R., Carey, S. K., Laudon, H., McDonnell, J., McGuire, K., Seibert, J., and Shanley, J.: Catchments on the cusp? Structural and functional change in northern ecohydrology, Hydrol. Process., 27, 766-774, https://doi.org/10.1002/hyp.9700, 2013.

Xiao, W., Wei, Z., and Wen, X.: Evapotranspiration partitioning at the ecosystem scale using the stable isotope method—A review, Agr. Forest Meteorol., 263, 346-361, https://doi.org/10.1016/j.agrformet.2018.09.005, 2018.

Yin, L., Dai, E., Zheng, D., Wang, Y., Ma, L., and Tong, M.: What drives the vegetation dynamics in the Hengduan Mountain region, southwest China: Climate change or human activity? Ecol. Indic., 112, 106013, https://doi.org/10.1016/j.ecolind.2019.106013, 2020.

Zhu, G., Yong, L., Zhang, Z., Sun, Z., Sang, L., Liu, Y., Wang, L., and Guo, H.: Infiltration process of irrigation water in oasis farmland and its enlightenment to optimization of irrigation mode: Based on stable isotope data, Agr. Water Manage., 258, 107173, https://doi.org/10.1016/j.agwat.2021.107173, 2021a.

Zhu, G., Yong, L., Zhang, Z., Sun, Z., Wan, Q., Xu, Y., Ma, H., Sang, L., Liu, Y., Wang, L., Zhao, K., and Guo, H.: Effects of plastic mulch on soil water migration in arid oasis farmland: Evidence of stable isotopes, Catena, 207, 105580, https://doi.org/10.1016/j.catena.2021.105580, 2021b.

Zimmermann, U., Münnich, K. O., Roether, W., Kreutz, W., Schubach, K., and Siegel, O.: Tracers Determine Movement of Soil Moisture and Evapotranspiration, Science, 152, 346-347, https://doi.org/10.1126/science.152.3720.346, 1966.

Acknowledgments

This research was financially supported by the National Natural Science Foundation of China (41661005, 41867030, 41971036). The authors much thank the colleagues in the Northwest Normal University for their help in fieldwork, laboratory analysis, data processing.

Author Contribution statement

Guofeng Zhu and Leilei Yong conceived the idea of the study; Yuanxiao Xu and Qiaozhuo Wan analyzed the data; Zhigang Sun and Leilei Yong were responsible for field sampling; Zhuanxia Zhang participated in the experiment; Lei Wang participated in the drawing; Leilei Yong wrote the paper; Liyuan Sang, Xi Zhao and Yuwei Liu checked and edited language. All authors discussed the results and revised the manuscript.

Additional Information

Competing Interests: The authors declare no competing interests.